Nonlin. Processes Geophys., 14, 1–13, 2007
www.nonlin-processes-geophys.net/14/1/2007/

Nonlinear Processes in Geophysics

Percolating magmas in three dimensions

H. Gaonac'h[1], **S. Lovejoy**[1,2], **M. Carrier-Nunes**[1,2], **D. Schertzer**[3,4], **and F. Lepine**[2]

[1]GEOTOP-UQAM/McGill Centre, UQAM, Montreal, Qc., Canada
[2]Physics, McGill, 3600 University st., Montreal, Qc. H3A 2T8, Canada
[3]CEREVE, ENPC, 6–8, avenue Blaise Pascal, Cité Descartes, 77455 Marne-la vallée, Cedex, France
[4]Meteo France, 1 Quai Branly, 75007 Paris, France

Received: 19 March 2007 – Revised: 27 July 2007 – Accepted: 6 September 2007 – Published:

Abstract. The classical models of volcanic eruptions assume that they originate as a consequence of critical stresses or critical strain rates being exceeded in the magma followed by catastrophic fragmentation. In a recent paper (Gaonac'h et al., 2003) we proposed an additional mechanism based on the properties of complex networks of overlapping bubbles; that extreme multibubble coalescence could lead to catastrophic changes in the magma rheology at a critical vesicularity. This is possible because at a critical vesicularity P_c (the percolation threshold), even in the absence of external stresses the magma fragments. By considering 2-D percolation with the (observed) extreme power law bubble distributions, we showed numerically that P_{2c} had the apparently realistic value $\approx$0.7.

The properties of percolating systems are, however, significantly different in 2-D and 3-D. In this paper, we discuss various new features relevant to 3-D percolation and compare the model predictions with empirical data on explosive volcanism. The most important points are a) bubbles and magma have different 3-D critical percolation points; we show numerically that with power law bubble distributions that the important magma percolation threshold $P_{3c,m}$ has the high value $\approx 0.97 \pm 0.01$, b) a generic result of 3-D percolation is that the resulting primary fragments will have power law distributions with exponent $B_{3f} \approx 1.186 \pm 0.002$, near the empirical value (for pumice) $\approx 1.1 \pm 0.1$; c) we review the relevant percolation literature and point out that the elastic properties may have lower – possibly more realistic – critical vesicularities relevant to magmas; d) we explore the implications of long range correlations (power law bubble distributions) and discuss this in combination with bubble anisotropy; e) we propose a new kind of intermediate "elliptical" dimensional percolation involving differentially elongated bubbles and show that it can lead to somewhat lower critical thresholds.

These percolation mechanisms for catastrophically weakening magma would presumably operate in conjunction with the classical critical stress and critical strain mechanisms. We conclude that percolation theory provides an attractive theoretical framework for understanding highly vesicular magma.

Correspondence to: H. Gaonac'h
(gaonach.helene@uqam.ca)

1 Introduction

Bubbles play a crucial role in controlling the style and intensity of volcanism: when reaching a free surface they can relieve pressure – possibly violently – and when they are trapped in the ascending magma, they can weaken its structure. In order for this weakening to lead to an explosive rather than an effusive eruption style, one assumes that the system responds discontinuously/catastrophically to a small increase in some physical parameter. Two main fragmentation mechanisms are proposed. The first supposes that the bubble gas pressure increases sufficiently to overcome the tensile strength of the surrounding magma (e.g. Aldibirov, 1994; Zhang, 1999; Alidibirov and Dingwell, 1996); whereas the second is based on the idea that viscous strain rates could become higher than the relaxational strain rate of the melt (Dingwell and Webb, 1989; Papale, 1999). In both cases, the rheology changes catastrophically even though a physical parameter (gas pressure or strain rate) may only change by the (possibly) small amount necessary to exceed a threshold. The theoretical calculations underlying these models invariably make artificial assumptions about the geometry of bubbly magma such as ignoring multibubble interactions, assuming regular arrays of non-overlapping bubbles, the sphericity of bubbles, etc. While these assumptions may be valid at low vesicularities, they become questionable at larger ones where extreme bubble – bubble "overlap" and interaction must occur.

In all cases, the role of bubbles is important; recent advances in their understanding include studies of textural aspects of volcanic products issued from bubbly magmas

Published by Copernicus Publications on behalf of the European Geosciences Union and the American Geophysical Union.

Table 1. Definitions of variables used in the text.

P	Vesicularity of the magma
P_{ex}	Vesicularity at explosion
$P_{3c,b}$, $P_{3c,m}$, P_{2c} (or $P_{2c,b}$)	Critical vesicularity at percolation in a system. The subscript indicates the dimensionality, "b" indicates "bubbles", "m" magma"
A^*, V^*	The area and volume of largest bubbles (this diverges at P_c)
$n(A)$, $n(V)$	Number density of bubbles with areas between A and $A+dA$, (with volumes between V and $V+\mathrm{d}V$ in 3-D)
B_2, B_3	Initial bubble size distribution scaling exponent in 2-D and 3-D, respectively
B_{3f}	Universal fragmentation exponent in 3-D, valid near $P_{3c,m}$
V_{ex}, $<V_{ex}>$	Effective excluded volume, ensemble average of the effective extruded volume
$P_{2e,BB}$, $P_{2e,CF}$, $P_{3e,BB}$, $P_{3e,CF}$	Critical bond occupation fraction for central force (CF) and bond bending (BB) elasticity on lattices, the number indicates the dimensionality
L	Linear size dimension of the system
D_{el}=2+H_z	Elliptical dimension

(Klug and Cashman, 1994; Polacci et al., 2001; Klug et al., 2002; Gaonac'h et al., 1996a, b, Lovejoy et al., 2004); these studies have brought out the importance of coalescence and anisotropy of bubbles. Laboratory studies were also important for refining theories of magma fragmentation, especially Ichihara et al. (2002), Spieler et al. (2004), Namiki and Manga (2005, 2006). At an empirical level, Spieler et al. (2004) have established that at least for low to moderate vesicularities (below ≈20%–30%), that for a fixed bubble overpressure, there is a roughly linear relation between the yield strength and the vesicularity P of the bubbly fluid (the critical overpressure is proportional to $1/P$; see Table 1 for parameter definitions). Although the authors do not discuss this in much detail, for large P, the yield strengths inferred from their experiments are seemingly nearly independent of P even if the relation is hard to discern due to the large experiment to experiment variability. Indeed it would be surprising if high vesicularity conditions could be successfully modelled without taking into account complex multibubble interactions.

In Namiki and Manga (2005), magma was simulated by a gum rosin solution. Over a large range of initial vesicularity and pressure differentials they conducted rapid decompression experiments. The effects of the decompression rates on the eruption styles of the bubbly elastic fluid was investigated, demonstrating the important role of bubbles and deformation during expansion of the magma. In Namiki and Manga (2006) the effects of decompression rate on expansion style and velocity of the bubbly fluids were explored when viscosity was low enough to allow the expansion of the bubbles.

The classical eruption models focus on the consequences of the variation of external parameters on a relatively static magma; it is implicitly assumed that, for a given bubble overpressure, the rheology (e.g. the critical yield strength) evolves smoothly with vesicularity P (e.g. in Spieler et al., 2004, it evolves linearly with P). Yet there are reasons to believe that the relation may not always be smooth and can even be singular. This is because it is generally acknowledged that explosions typically occur at such high vesicularities P_{ex} that the bubbles necessarily overlap into complex networks. For example, Sparks (1978) suggests that at the moment of explosion P_{ex}≈75–77% is quite common and Gardner et al. (1996) finds P≈0.64 for eruption products coming from magmas with viscosities higher than 10^5 Pa s. Since the most vesicular products (more fragile) are more susceptible to secondary fragmentation this is presumably a lower bound on P_{ex} (see below).

The geometry of idealized versions of these bubble networks – in which all the bubbles are placed uniformly at random and have various distributions of shapes and orientations – has been extensively studied in statistical physics; the problem of "percolation" (see Stauffer, 1985, for an introduction). Percolation theory shows that under fairly general circumstances the superposition of such randomly distributed shapes results in a geometric phase transition around a critical vesicularity P_c. Applied to bubbles, this means that as the vesicularity P approaches P_{2c}, (P_{3c} in 3-D) the area A^* (or volumes V* in 3-D) of the largest simply connected bubbles diverges:

$$\begin{array}{l} A^* \approx |P - P_{2c}|^{-2\nu_2} \text{ ; 2-D} \\ V^* \approx |P - P_{3c}|^{-3\nu_3} \text{ ; 3-D} \end{array} \quad (1)$$

(ν is the "correlation length exponent"; ν_2=4/3 (Den Nijs, 1979); ν_3=0.88±0.02 (Grassberger, 1983). In a 2-D system the largest bubble spans the system and effectively cleaves it in half so that even if there is no external stress, at P_{2c} the magma is reduced to a collection of disconnected fragments. In Gaonac'h et al. (2003), this singular behaviour of percolating systems was used as the basis of a critical rheological model for explosive volcanism in which the stresses and strain rates play only passive roles, but in which the vesicularity plays the role of critical parameter: in a stressed magma, if P slowly rises to the critical value P_{2c} catastrophic fragmentation will result. Although it is possible that certain volcanic explosions are purely consequences of this bubble-based mechanism, the percolation mechanism is clearly not in contradiction with the classical mechanisms. Indeed volcanic explosions may occur because the percolation point is reached in some particularly porous part of the magma column which then breaks down locally. This local breakdown could create a pressure wave that disrupts the surrounding magma by classical critical stress mechanisms.

The most commonly discussed type of percolation is that which occurs on a regular lattice. In contrast, the bubble percolation we proposed is a type of "continuum percolation" which is theoretically and numerically harder to investigate. General percolation theory predicts that the percolation exponents (ν_D in Eq. (1), D is the dimension of space; there are other exponents including a fragmentation exponent; see below) are "universal" in the sense that they are the same for virtually any basic shape in both lattice and continuum percolation. However, the critical P_c is not universal and is usually determined numerically and after considerable effort.

While standard continuum percolation theory uses "monodisperse" distributions (all the basic shapes are the same size), in order to apply percolation theory to a bubbly magma, it was on the contrary proposed that a wide power law distribution of basic bubble sizes should be used. This was justified on the one hand because the basic bubble-bubble (binary) coalescence mechanism has no characteristic size and hence leads to power law distributions of gas vesicles (Gaonac'h et al., 1996b; Lovejoy et al., 2004). On the other hand it was justified empirically; Gaonac'h et al. (1996a), Klug et al. (2002) found:

$$\begin{array}{l} n(A) \approx A^{-B_2-1};\ \text{2-D} \\ n(V) \approx V^{-B_3-1};\ \text{3-D} \end{array} \quad (2)$$

where n is the number density of bubbles with areas between A and $A+dA$, (with volumes between V and $V+\mathrm{d}V$, in 3-D); empirically they found $B_2 \approx 0.75$. This is quite an extreme distribution indeed, since whenever B_2 or $B_3 < 1$ it is so dominated by the large bubbles that a cut-off is needed (here taken as a fixed fraction of the system size) in order to stop the mean diverging in the large bubble limit (this is necessary so that the model can be normalized to yield a finite mean vesicularity). According to the terminology of de Dreuzy et al. (2000) power law percolation is a "long-range" rather than a "short-range" type where all bubbles would be smaller than the size of the magmatic system. Figure 1 demonstrates that the observed power law percolation is in the same "universality" class as the usual monodisperse percolation (same invariant ν_2 exponent) since it is well fit by the theoretical universal monodisperse exponent ν_2=4/3 (Den Nijs, 1979). Using this power law distribution and B_2=0.75 on numerical simulations, (Gaonac'h et al., 2003) found $P_{2c} \approx 0.7 \pm 0.05$ which is quite close to the vesicularity (Sparks, 1978; Gardner et al., 1996) observed in the products of explosive volcanism.

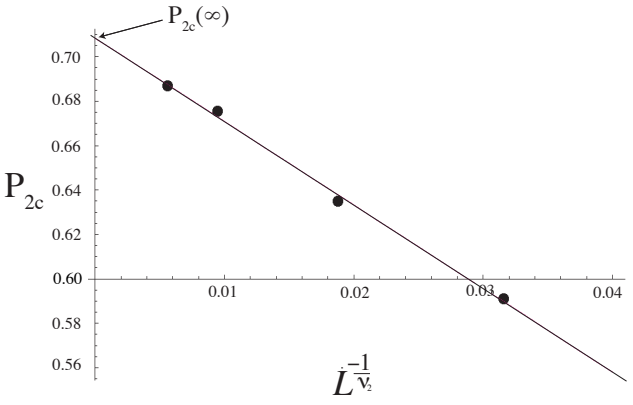

Fig. 1. This shows an accurate estimate of the infinite system 2-D percolation threshold P_{2c} for power law bubble distributions from simulations. The scale invariant exponent used in the numerical simulation is B_2=0.75 (the empirical value). The (finite sized) percolation threshold is estimated at four different sized systems L=2^7, 2^8, 2^9, 2^{10} and then plotted against $L^{\frac{-1}{\nu_2}}$ where ν_2=4/3 is the theoretical correlation length exponent; this is a standard method for dealing with finite size effects. The extrapolation of $L^{\frac{-1}{\nu_2}}$ to zero yields the infinite system percolation threshold; here P_{2c}=0.708±0.001. This is close to the approximate value 0.70±0.05 cited in Gaonac'h et al. (2003). The largest bubbles in the initial distribution had diameters =10% of the system size.

Unfortunately, the more realistic 3-D case was not considered. At the time, it appeared that the change in the 2-D percolation threshold resulting from the replacement of monodisperse by power law bubble distributions was very considerable. According to data in the review (ben-Avraham and Havlin, 2000), (Table 2.1, p. 17) the monodisperse 2-D P_{2c} had the value 0.312±0.005 which was only slightly above the 3-D value 0.2895±0.0005 (Rintoul and Torquato, 1997). It was therefore concluded that the dimensionality did not have a strong influence on P_c, and that the increase from $P_{2c} \approx 0.3$ (monodisperse) to 0.7 (power law) was due to the strong effect of the power law bubble distribution. Unfortunately, the review value P_{2c}=0.312±0.005 turned out to be a misprint; the correct (and up to date) value is P_{2c}=0.676339±0.000004 (Quintanilla, 2001). In reality, the bubble distribution only has a small effect on P_c (see however Sect. 5) whereas the effect of the dimension of space is

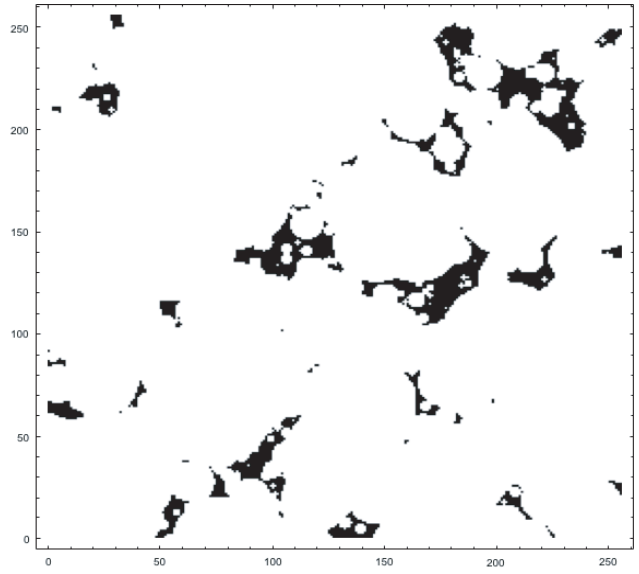

Fig. 2a. A horizontal section through a 256^3 power law (B_3=0.85) system just below the magma percolation point at $P_{3c,m}$=0.97. Bubbles are white; the rocky matrix/viscous magma is black. Most of the bubbles are actually joined via connections out of the plane.

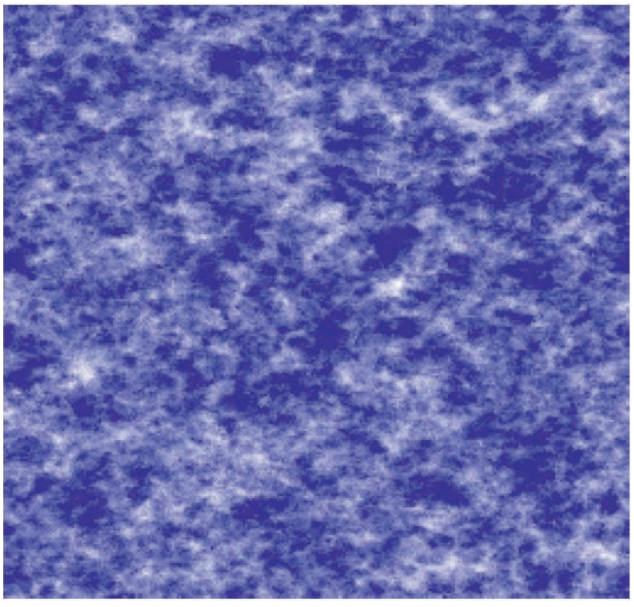

Fig. 2b. A "cloud" rendition of the previous simulation bringing out the filamentary nature of the magma near the magma percolation point. Here, the intensity (white to saturated blue) depends on the exponentially weighted total (integrated) magma density along a column perpendicular to the surface, the brighter regions are those where most light would pass if lit from the other side, i.e. a representation of gas bubbles.

very large. Indeed, a much more precise calculation of P_{2c} in the case of power law bubbles (see Fig. 1) taking into account the size of the finite simulated system shows that the infinite system has a value of P_{2c}=0.708±0.001, so that the effect of changing the distribution – even for a distribution as extreme as a power law distribution with $B<1$ – is actually fairly small. Due to the much lower monodisperse 3-D P_{3c} value, it is therefore important to re-examine the percolation model of explosive volcanism. On the one hand, we seek to verify the effect of power law bubble distributions in 3-D (in particular on the value of P_{3c}), on the other, we explore some new features of 3-D percolation not present in 2-D and some implications for volcanic systems.

2 3-D continuum percolation: power law and monodisperse bubble distributions

Percolation in 2-D is relatively straightforward. Below P_{2c}, the largest bubble is of finite extent (A in Eq. 1), the surrounding magma region is infinite and "magma" percolation prevails (a path is possible from one side of the system to the other without crossing through bubbles). At P_{2c} a percolating network of bubbles is formed (a path is possible from one side of the system to the other only through bubbles). This path cleaves the magma into finite sized fragments; the overall system will therefore lose its tensile strength. The point P_{2c}, is critical for both geometric and rheological properties. In 3-D the situation is more complicated, there are two different percolation thresholds: the percolation threshold of the gas bubble

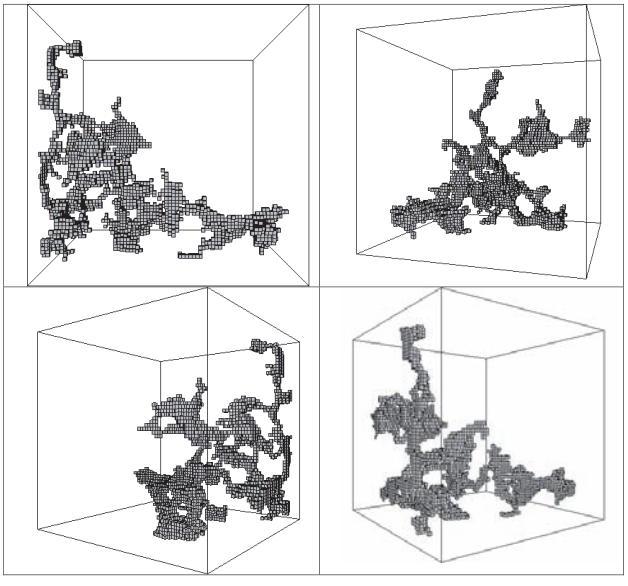

Fig. 2c. Four different view angles showing a simulation of the percolating magma cluster (largest magma fragment – in grey) with power law bubble distribution (B_3=0.85) on a 64^3 simulation showing the extremely fragile and complex created structures at such high vesicularity (P=0.95).

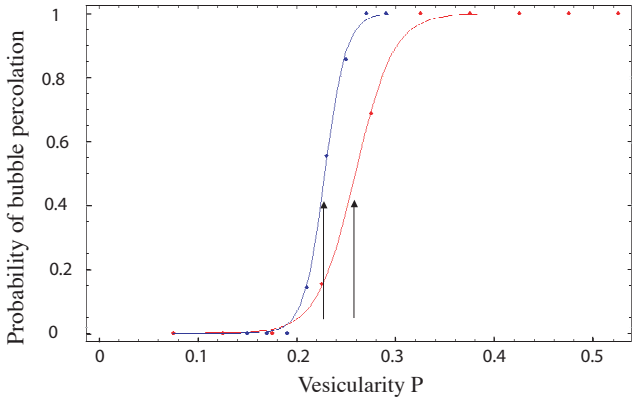

Fig. 3a. This shows the probability of bubble percolation as a function of vesicularity of the system for power distributed spheres, B_3=0.85 (blue) and monodisperse (red). The simulations were made on 256^3 grids, in the monodisperse case, the radii were 10 pixels, in the power law case, the large bubble cut-off on the initial distribution had radius 10 pixels; there were about 100 simulations in each case. The curves are fits to the semi-empirical function $^1/_2$ (1+tanh $a(P-P_c)$) where a is a constant (determined by the finite size of the system). The arrows show the values of P_c estimated here as $P_{3c,b}$=0.228, 0.259 for the power law and monodisperse systems, respectively. The latter is slightly below the literature (infinite system) value 0.2895±0.0005 due to finite size effects.

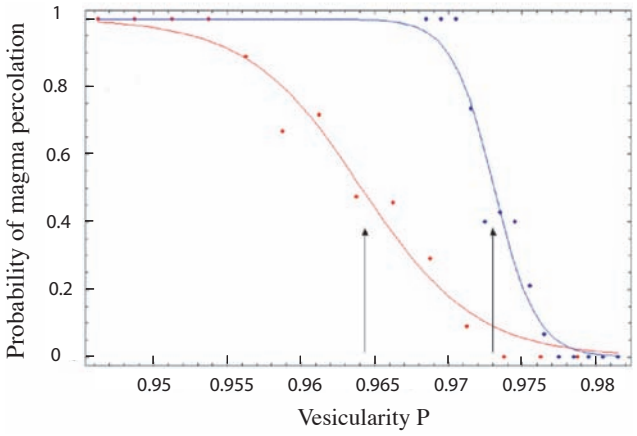

Fig. 3b. Same as Fig. 3a except for magma percolation. $P_{3c,m}$=0.973, 0.964 for the power law (blue) and monodisperse (red) respectively bubbles. There were about 120 simulations in each case. Again the monodisperse value is slightly different from the literature (infinite) system value due to finite size effects.

network, $P_{3c,b}$, and the percolation threshold of the surrounding magma, $P_{3c,m}$ (the subscript "*b*" for "bubbles", "*m*" for "magma"). At the critical $P_{3c,b}$=0.2895±0.0005 for monodisperse spheres (Rintoul and Torquato, 1997), there is a continuous spaghetti-like fractal bubble spanning the system, but the magmatic surrounding matrix is – with the exception of a few small fragments – all connected, infinitely large and percolating. However when one reaches a much higher vesicularity $P_{3c,m}$≈0.9699±0.0003 (Rintoul, 2000), the magma fragments i.e. the magma stops percolating; this is another critical threshold with the same "universal" exponents. For lattice percolation Grassberger (1983) finds ν_3=0.88±0.02 for continuum percolation while Rintoul (2000) gives ν_3=0.902±0.005 (the two are presumed to be the same to within numerical error). Figures 2a, b, c exhibit the fragile filamentary magmatic structures at this high vesicularity.

In the continuum percolation literature, it is traditional to consider that the complement of the percolating elements are "voids". In applications to magmas, this can be confusing since the percolating medium is a gas bubble, the complement being the viscous magma – or when analysing volcanic samples – the solid matrix and crystals. The magma percolation cited above is therefore called "void percolation" or "Swiss cheese percolation". Although void percolation hasn't attracted so much attention, Yi (2006) has investigated the effect of changing the shape of the basic elements from spheres to ellipsoids. On 1200^3 grids, he showed that increasing the elongation ratio of the (monodisperse) ellipses to 8:1 (the maximum possible on his grid) $P_{3c,m}$ decreased by about 1% from the spherical value $P_{3c,m}$≈0.9699±0.003 (Rintoul, 2000), to $P_{3c,m}$≈0.958. This is in contrast with our simulations in Fig. 3b indicating about a 1% increase in $P_{3c,m}$ when monodisperse distributions of spheres are replaced by power law distributions with B_3=0.85. As pointed out in Gaonac'h et al. (2003), if B_2 is the bubble size exponent of a 2-D cross-section of an isotropic 3-D percolation process, then when passing from 2-D to 3-D we must use the relation $2(1-B_2)=3(1-B_3)$ so that the empirical B_2=0.75 corresponds to B_3≈0.85.

For the percolating model of explosive volcanism, this second $P_{3c,m}$ is the most important in the sense that it is at this very high level of vesicularity that the magmatic system is completely fragmented, where the tensile strength of the magma completely vanishes. If the system is under stress and just below $P_{3c,m}$, then an imperceptible increase in P leads to a catastrophic weakening of the system and hence explosion. In comparison, at $P_{3c,b}$ while degassing will be enhanced by the percolating bubble network, the magma rheology will only change imperceptibly and the magma would continue its ascent without being too disturbed. Unfortunately, the value $P_{3c,m}$ is quite high, perhaps too high to be compatible with the observations although – as discussed below – the observations on explosive products may not be straightforward to interpret. This is especially true since it may be enough for a localized region to reach the percolation threshold in order to provoke first a local and then a more general fragmentation. Before discussing this further, let us first check that changing from a monodisperse to power law distribution does not alter the P_{3c}'s very much. Figures 3a, b show the results of numerical simulations for estimating a

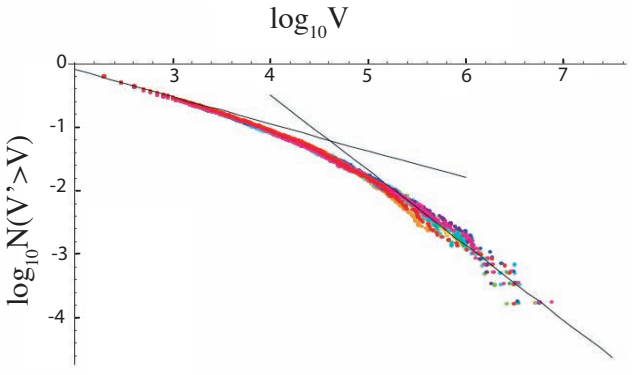

Fig. 4a. This shows the fragment distribution of 11 non percolating simulations on 256^3 lattice involving power law bubble distributions with B_3=0.85 taken at P=0.967 (near $P_{3c,m}$). The distributions are normalized by the total number of bubbles so that the ordinate is actually the relative probability of fragments of a given volume. The reference slopes have the theoretical universal percolation value $B_3/2$=0.425 (left) and 1.186 (right). The latter formula was also found in 2-D simulations in Gaonac'h et al. (2003) but the formula $B_3/2$ is only semi-empirical.

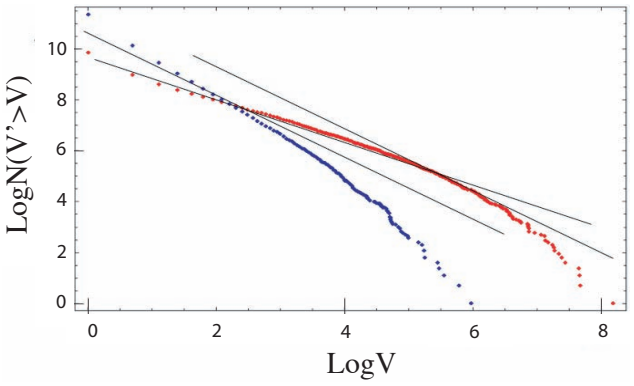

Fig. 4b. This shows the average number distributions of volcanic fragments from 600 simulations sized 128^3 for both monodisperse (blue) and power law (red) percolation at a P value of 0.7, i.e. below the $P_{3c,m}$ value (note; B_3=0.85 was used for the bubble distribution and natural logs are used on the graph). The radius of the monodisperse bubbles was 10 pixels, the largest bubble in the power law simulations was also 10 pixels in radius. This corresponds to a Log(volume)=8.34 corresponding to a characteristic scale that breaks the scaling (note the base e here). The two steep reference lines have slopes -1.186. The shallow reference line has slope -0.85. While the second exponent is the universal prediction of continuum percolation theory for P close to $P_{3c,m}$, the former behaviour (0.85) is nontrivial to explain since it is the bubble distribution which has a power law with B_3=0.85. Since these simulations were below $P_{3c,m}$, the single largest fragments on each simulation percolate and were removed from the distributions.

monodisperse and power law distribution with B_3=0.85. We can see that not only are the finite monodisperse P_{3c}'s close to the theoretical infinite system values ($P_{3,m}\approx$0.964 – see Fig. 3b – i.e. to within 0.6% of the value 0.9699±0.0003 (Rintoul, 2000); this serves as a check on the simulations), but also that the power law simulations are not very different, with $P_{3c,b}$ about 3% lower and $P_{3c,m}$ about 1% higher than the corresponding monodisperse values. Although we did not attempt to extrapolate these 256^3 values to infinite system values, the difference is small and is expected to persist in the limit (see the discussion in Sect. 5).

A seductive feature is that this model elegantly explains the fragment size distributions observed for pumice. One of the universal features of percolation at the critical point is indeed the existence of a power law distribution of fragments with universal percolation exponent in 3-D, $B_{3f}\approx$1.186±0.002 (Jan and Stauffer, 1998); "f for "fragment"; $B_{3f}=\tau-1$ where τ is the usual percolation notation. Our simulations confirmed that the power law bubble distributions did not alter this value (Fig. 4a) which is very close to the empirical value $B_{3,f}\approx$1.1±0.1 from Plinian fragments (Kaminski and Jaupart, 1998). Note that in some of the literature (e.g. Kaminski and Jaupart, 1998; Kueppers et al., 2006) the exponent $3B_{3f}$ is used instead. It is denoted by the symbol D and is incorrectly referred to as a "fractal dimension" even though it is not the fractal dimension of any set of points; indeed, since $3B_{3,f}>3$, it could not possibly represent a set embedded in three-dimensional space. This value $B_{3f}>1$ contrasts with the much smaller value obtained in 2-D percolation ($\approx B_2/2$; see Gaonac'h et al., 2003, for a discussion). In addition, as noted by Kaminski and Jaupart (1998) values of $B_{3f}>1$ cannot be obtained by simple classical fragmentation mechanisms (they suggested a series of fragmentation events happening in the eruptive column) so that the 3-D percolation explanation for $B_{3f}>1$ is particularly appealing. We should note that this power law distribution tail only appears near $P_{3c,m}$ (≈90%); however Fig. 4b shows that somewhat below this value ($P_{3c,m}$=0.7), in the power law (but not monodisperse case) this theoretical behaviour may already be starting to be visible.

3 3-D continuum percolation as a model for explosive volcanism

We have noted that in the absence of external stress, complete fragmentation of the magma will only occur near the relatively high (monodisperse) value $P_{3c,m}\approx$0.9699. While this seems high, it is worth noting that the evidence for the critical explosive vesicularity P_{ex} being around 0.6–0.7 is indirect, being based on the vesicularity of eruption products. However, according to the percolation model, while the overall magma may have a large P at the moment of explosion, the individual fragments will have a distribution of P values each of which will be quite a bit lower, possibly quite close to observations. In addition, after the explosion some of the volcanic products will stay hot longer so that the bubbles inside

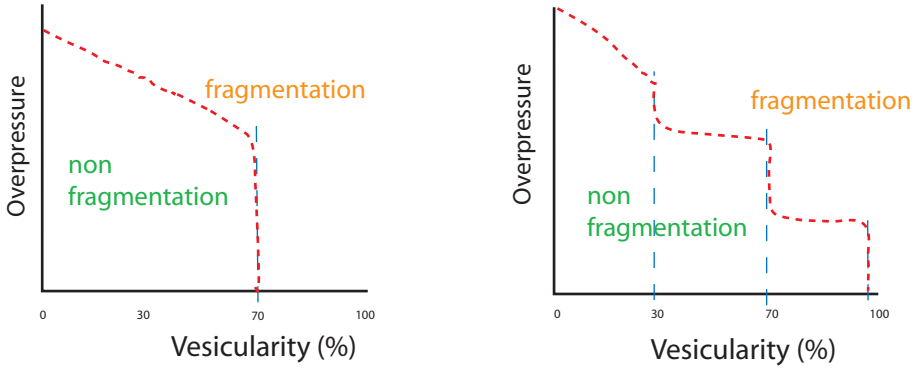

Fig. 5. Schematic diagrams showing the hypothetical response of porous magma to pressure gradients at varying values of P (ordinates, in percentage).

each fragment will continue to expand and coalesce and – presumably in some cases – continue to fragment after the initial explosion, e.g. Thomas et al. (1994). While this makes it difficult to infer the P_{ex} in the magma at the moment of the explosion it does not necessarily change the overall bubble size distributions.

Even with these caveats, real magmas are under stress and will certainly fragment below $P_{3c,m}$. The problem is to determine how the rheology – in particular the yield strength – of the magma evolves with P. While the percolation model may indeed provide a good approximation to the magma geometry – since it is a fairly general model of multibubble overlap (and we hypothesize, multibubble coalescence) – in itself it will explain explosive volcanism only if for some relevant small range of vesicularity P, the rheology varies extremely rapidly. While we postpone a discussion of the mechanical properties of percolating systems to a later section, we can use our knowledge of 2-D and 3-D percolation to make a schematic of the plausible behaviour of the bubbly viscoelastic fluid (Fig. 5). On the left we see the relatively simple situation in 2-D where a single percolation threshold exists. As the vesicularity increases from 0% to 70%, less and less overpressure is needed to fragment the system. At P_{2c} (close to 70%) fragmentation occurs even at vanishing surrounding pressure gradients. On the right, we see the situation in 3-D where there are several critical P values associated with abrupt changes in the yield strength of the magmatic system. Starting at low vesicularity, we hypothesize that when P exceeds first $P_{3c,b}$ ($\approx$30%) – where the bubbles form infinite spaghetti-like fractal networks and allow more effective degassing – there may be a corresponding weakening of the still percolating magma. Then, at $P=P_{2c}$ ($\approx$70%) every planar cross-section will undergo 2-D bubble percolation, hence every plane will be cleaved by an infinite sized bubble. We hypothesize that this might cause further rapid weakening of the magmatic rheology near this value, possibly explaining the common observations of P near 70% in the volcanic products. Finally, at $P_{3c,m}$ ($\approx$97%) – and this is not speculation but a sure consequence of 3-D percolation – the entire magma fragments (the magma no longer percolates) even in the absence of a surrounding pressure gradient.

We have seen that due to 2-D percolation catastrophically cleaving every planar section at $P_{2c}\approx$0.708, it is possible that the rheology of the magmatic system will respond abruptly even at values well below $P_{3c,m}$. Figure 4b shows that – at least in the case of power law bubble distributions – that the primary fragments have size distributions with long tails not too far from the theoretical power law with exponent B_{3f} (hence close to the observations of Kaminski and Jaupart, 1998). The only direct way to test this model would be either empirically by testing the yield strengths of volcanic products as functions of their vesicularities (something which to our knowledge has not yet been done systematically), or to perform (difficult) numerical or theoretical calculations on percolating systems (see however below). Probably the best relevant information currently available is from laboratory experiments by Namiki and Manga (2005) (see Fig. 6) which although not conclusive do seem compatible with the percolation based schematic Fig. 5. The authors conducted rapid decompression experiments of an analogue of a bubbly magma varying the initial vesicularity and pressure change from one experiment to another. They observed various patterns in response to the experimental conditions such as "fragmentation" or "partial rupture" regimes and plotted the estimated observed experimental values in hypothesized regions in accordance to initial vesicularities, pressure changes and potential energy (assumed to be transformed into kinetic energy). In order to interpret Fig. 6 in terms of the percolation model, two points must be borne in mind. First, while the percolation model applies to the vesicularity at the moment of fragmentation, Fig. 6 refers to the initial vesicularity i.e. just before a sudden decompression – expansion of the bubbles. In spite of this, we may note from the figure that – as expected (cf. Fig. 5) – when $P>70\%$ the pressure gradient need not be very high to cause rupture and fragmentation. At $P_{3c,m}\approx$95% the system will fragment as discussed

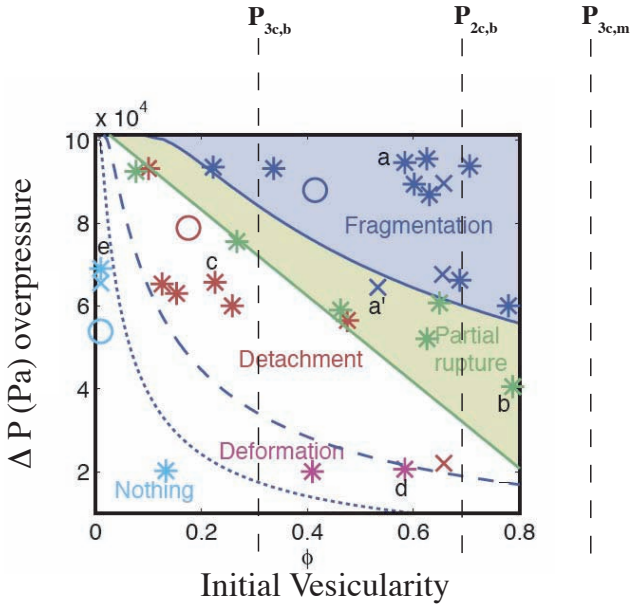

Fig. 6. A "regime" diagram of laboratory observed bubbly magma behaviour as a function of initial vesicularity ϕ and overpressure ΔP. The various symbols represent different experimental conditions; adapted from Namiki and Manga (2005). The three vertical lines show the three different 3-D percolation thresholds identified in the present paper as critical vesicularities relevant to magmatic rheology (see Fig. 5). Blue, green, red, pink and light-blue symbols show cases with fragmentation, partial rupture, detachment, deformation and "nothing". See Namiki and Manga (2005). Crosses, circles and asteriks indicate different concentrations of their experimental solutions. Their diagram is divided in five distinct expansion styles (see Namiki and Manga, 2005, for explanations).

above. Second, in addition to the nontrivial relation between initial vesicularity and the vesicularity at the moment of fragmentation, the straightforward application of the percolation model to explosive volcanism is under slowly varying conditions with vesicularity P slowly rising – and not under rapid decompression. Such depressurization – at least in local planar regions perpendicular to the pressure change variation – is particularly favourable to fragmentation (Ichihara et al., 2002) so that in addition to visco-elastic extensions of the theory we must also take into account anisotropy.

4 Magma Rheology and critical elastic properties in percolating systems

Magmas are viscoelastic fluids implying that viscous and elastic properties of the fluid depend on the relevant expansion and decompression rates (see Ichihara et al., 2002). While it is possible that 3-D percolation as described above is already an adequate model of explosive volcanism, it is worth exploring other avenues for obtaining singular behaviour at lower more commonly observed P_c's than 90%. If we approximate the magma as an elastic solid, then we may be able to apply the theoretical results on the elastic properties of percolating systems that have been studied since the 1980s. The key result (Arbabi and Sahimi, 1988, 1993; Sahimi and Arbabi, 1993; and see the discussion in Craciun et al., 1998) is that there are two different universality classes (implying in each class a specific critical vesicularity threshold) for the elastic properties depending on whether the interacting elements (e.g. the bonds between the sites in bond percolation) have elastic properties only along the lines connecting the sites ("central force", the CF model), or with resistance tangential to this line ("bond bending", the BB model).

To understand why there might be differences between CF and BB elasticity, consider the simple example of bond percolation on a square lattice in 2-D. In the pure CF model, each bond is a spring; however since the springs cannot resist tangential forces, even if all bonds are present (the fraction of bonds =1), the entire lattice will "flop" over with even an infinitesimal tangential push. On the contrary, in the pure BB model, we may think of each bond as a flexible beam rather than a spring, and as the fraction of bonds decreases, the structure will maintain its integrity until the geometric phase transition occurs at the usual percolation threshold of the bond network (which is exactly $1/2$ in this case (Essam et al., 1978)). In this example, the critical CF point of the lattice is $P_{2e,CF}$=1, whereas the critical BB point is $P_{2e,BB}$=1/2 ("e" for "elastic" critical threshold). Clearly we generally have $P_{e,CF} \geq P_{e,BB}$; and in lattices (such as the triangular lattice) where $P_{2e,CF}$ exceeds $P_{2e,BB}$, if we start at a bond fraction of 100% and decrease it, we find that the structure - although still geometrically percolating – catastrophically loses its ability to resist stresses at $P_{2e,CF}$. In real materials of course there will generally be a mixture of CF and BB, (this is called a "cross-over" behaviour) so that the BB elasticity will ultimately be dominant at large enough scales. However if the BB contribution is small, the structure can still weaken rapidly at the critical CF percolation point $P_{3e,CF}$.

If we consider the results on 3-D elastic properties, we find that the critical threshold in the 3-D bond bending model – the point where there is a singularity in the elastic modulii $P_{3e,BB}$ – is low (in most models it is equal to the corresponding $P_{3c,b}$ i.e. around 20–30%; we use the subscript "b" although in this lattice model the bubble analogue is a spring/elastic bond). What is notable is that the 3-D central force model has much higher values $P_{3e,CF}$ than $P_{3e,BB}$. For example, in (3-D) body centred cubic lattices with bond percolation Arbabi and Sahimi (1993) find $P_{3e,CF}$=0.737±0.002.

However, before concluding that critical elastic properties could potentially explain critical magma rheology at such a high percolation threshold, it must be recalled that the percolation of a system is usually identified with the fraction of gas bubbles, not magma. The critical $P_{3e,CF}$ however corresponds to a fraction 0.737±0.002 of (central force

only) springs on a body centred cubic lattice, i.e. to the lattice analogue of 1–0.737±0.002=0.263±0.002 voids. In comparison, on the same body centred cubic lattice Lorenz and Ziff (1998) found for (bond bending only) springs $P_{3e,BB}=P_{3c,b}$=0.1802875 corresponding to the absence of springs on a fraction 0.8299125. However, we have seen from the example of continuum void percolation that we cannot simply take $P_{3c,b}=1-P_{3c,m}$ (the bubble percolation threshold is close to 30% while that of the magma is close to 90%); we must really do a proper elastic calculation on a continuum model with appropriate microscopic elastic properties, a difficult operation to conduct. At present, one uses lattice percolation with random individual elastic bonds distributed with a probability distribution which attempts to mimick the "necks" and other connectivity morphologies which arise in continuum percolation (the magmatic analogue would be the walls, plateaus and matrix of the magma system). Once the lattice elasticity calculation has been made, the equivalent continuum critical elastic threshold can be estimated using the lattice filling factor method of Scher and Zallen (1970). In other words, elastic threshold estimates that are directly relevant to percolating magmas (even ignoring viscous effects) do not exist and will require explicit modelling. For the moment, we conclude that the existing lattice based results are mostly suggestive, and that magma rheology requires much research.

Due to the difficulty of direct calculations, it is relevant to mention the laboratory results of Meille and Garboczi (2001) who compare numerical simulations and laboratory results on gypsum plaster. In at least one of their experimental systems, they find a critical elastic vesicularity $P_{3c,e}\approx 0.8$; they underline the difference between 2-D and 3-D behaviours and the importance of 3-D simulations for comparing with real world systems and point to mechanisms which could lower critical P values for magma rheology.

5 The effect of distributions of anisotropic percolation elements on the percolation threshold

The effect of distributions of anisotropic shapes (with a given distribution of orientation directions) has classically been treated using "excluded volume" theory. The idea is to take into account the fact that the degree of overlap of differently shaped elements (here, the bubbles) can be statistically accounted for, and that this determines the efficiency with which the elements can connect up. Based on this idea Balberg (1985) argued that in 3-D if the critical effective excluded volume is $<V_{ex}>$, then the bubble percolation threshold is $P_{3c}=1-e^{-\frac{<V_{ex}>}{8}}$. He then argued that for any distribution of shapes and orientations that $0.7\leq<V_{ex}><2.8$ (implying the bounds $0.08\leq P_{3c}\leq 0.29$). However, de Dreuzy et al. (2000) argued that this result does not apply in cases with wide power law size distributions (where for example, various statistical moments needed for the excluded volume calculation may diverge). They showed how to handle the excluded volume in this power law ("long-range correlations") case and with the help of numerical simulations, they calculated the effective excluded volumes and corresponding percolation thresholds for power law element distributions with $1/2\leq B_3\leq 4/3$ and with eccentricities $0.01\leq e\leq 1$. As B_3 decreases they found a generally increasing P_{3c}, a consequence of the stronger long-range correlations present at low B_3 where the system is increasingly dominated by a single large element (ellipses here) although some of this is probably due to finite size effects. Perhaps more interesting, is their finding that for fixed B_3, at eccentricities of around 0.5, P_{3c} reaches a maximum. For a given B_3 they considered the maximum P_{3c}'s, over all the eccentricities simulated. They found that this maximum P_{3c} varied monotonically over the range $0.33<P_{3c}<0.65$ as B_3 decreases from 4/3 to 1/2 (although their higher values of P_{3c} are subject to larger numerical uncertainty; these P values were calculated from their published excluded volume values). Using the experimental magma value B_3=0.85 their maximum $P_{3c,b}$ (obtained with their e=0.5) is 0.42. de Dreuzy et al. (2000) noted that using circular elements does not lead to such strong effects; however the effect of eccentricity is greatly enhanced by the long range correlation introduced by the power law distributions. In addition from their Fig. 5, we infer that $B_3\approx 0.85$ (corresponding to their a=2.6) is not low enough for very strong effects, in agreement with our results in Fig. 3a.

Caution should be taken before applying these results to 3-D magma percolation. Although de Dreuzy et al. (2000) used shapes with nonzero excluded volumes, they were interested in "fault" percolation and hence exclusively used 2-D shapes (circles, ellipses) with each having zero volumes. The results presented in our paper are apparently the first to consider finite volume percolating shapes with long range correlations. Assuming that the application of excluded volume theory is indeed correct, de Dreuzy et al. (2000) showed that by using power law distributions, it is possible to vary the percolation threshold over a somewhat wider range than previously believed. However with the exception of the limited results presented in Fig. 3b above, the effect of power law distributions on void percolation thresholds $P_{3c,m}$ has not been investigated. Nevertheless, it is interesting – at least for the spherical elements treated here – that with respect to the monodisperse value it increases rather than decreases the value of $P_{3c,m}$.

6 Other possibilities: stratified percolation with elliptical dimension between 2 and 3

The finding that percolation resulting from power law distributions of elements/bubbles is particularly effective at modifying the percolation threshold when it is combined with anisotropic shapes motivates further investigation of the role of the anisotropy of bubbles. Indeed, bubble shapes are

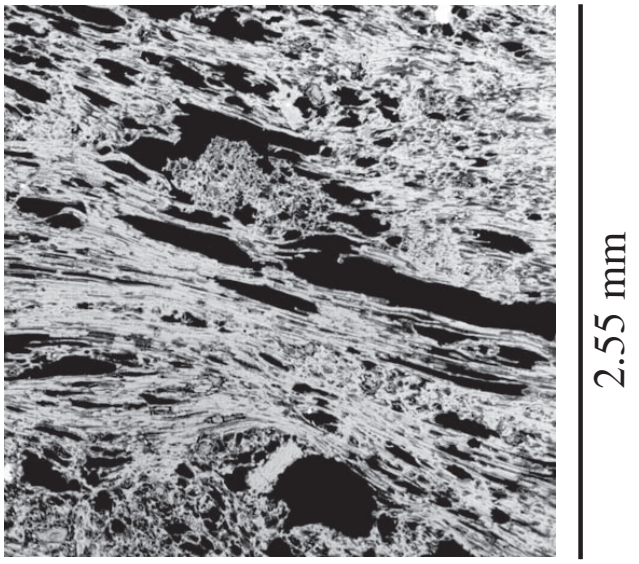

Fig. 7. Here is an example of a natural pumice displaying elongated large bubbles compared to less elongated smaller ones (from Santorini volcano). The image is a scanning electronic backscattered image. This image represents a Santorini volcano pumice.

highly non-spherical due to coalescence (Fig. 7; and Lovejoy et al., 2004) and magma stratification under stress (for example near the conduit walls). Evidence for this comes from the fragmented layers of elongated fragments found in flow banding perpendicular to the pressure gradient (e.g. Ichihara et al., 2002; Gonnermann and Manga, 2003; Namiki and Manga, 2005). If we have a power law bubble distribution, then it is both theoretically meaningful and physically plausible that the largest bubbles are the most "elongated" in the direction of shear; let us take this direction to be perpendicular to the z-axis and assume that the flattening occurs in the z-direction, so that in the x-y plane, bubbles have circular cross-sections size $\approx L$, but in the z-direction, they are flattened having extents $\approx L^{H_z}$ (with $0<H_z<1$). If the bubbles are spheres at L=1, then their $x-z$ or $y-z$ cross-sections will be ellipses with eccentricities increasing with L. The volumes of bubbles will therefore grow with L as Volume(L)$\approx L\times L\times L^{H_z}=L^{Del}$ where $2<D_{el}<3$ and $D_{el}=2+H_z$ is an "elliptical dimension"; see (Schertzer and Lovejoy, 1985). In this way the basic bubble structures can be made to interpolate between 2-D and 3-D. For example, in the limit of complete flattening into thin 2-D disks (H_z=0, D_{el}=2), the system will percolate from one side of the xy plane to the other at the 2-D percolation threshold P_{2c}. At the other extreme, (H_z=1, D_{el}=3) the shapes are spheres and we recover the 3-D $P_{3c,b}$. The reason that this system can be treated as having an intermediate dimension between 2-D and 3-D is because there is a power law distribution of bubble sizes leading to structures with increasingly flattening over a huge range of scales (indeed, it is only over this scale range that its effective dimension is D_{el}). In a monodisperse system, the flattening would in contrast have a relatively trivial effect since all the structures would be flattened by the same amount independently of their size.

From these extreme cases, we may expect that the percolation threshold will be different in the horizontal and vertical (z) directions. In addition, it is possible that the criterion for percolation may need to be appropriately changed with D_{el}. To get an idea of the problem, Fig. 8a shows a didactic example (without displaying the small bubbles) where we have taken H_z=0.6 (D_{el}=2.6). At a vesicularity of P=15% (Fig. 8b; H_z=0), the bubbles spread primarily on the xy plane. Even if we use the strict percolation criterion that $x-y$ percolation occurs only if a path exists across the system from a given z value to an identical z value on the other side, due to the connectivity in the z direction (Figs. 8b, c for H_z=0, D_{el}=2), we obtain percolation at a low value near $P_{3c,b}$ rather than the much higher P_{2c} (0.67). In this case, Fig. 8c shows the percolating bubbles: although their z direction spread is small, it is enough to drastically lower $P_{c,b}$.

To see how much differential anisotropy can affect the $P_{c,m}$ values, we show Fig. 9 with H_z=0.2, (i.e. D=2+H_z=2.2), B_3=0.85, which uses the standard percolation criterion but applies it to respectively the horizontal and vertical directions (H_z=0.2 is the lowest that can be reasonably simulated with a 200^3 lattice). The (finite system) percolation thresholds can be estimated by the fitting method of Fig. 3 yielding roughly $P_{2.2\mathrm{hor},c,m}$=0.916, $P_{2.2\mathrm{ver},c,m}$=0.893. These can be compared to the (isotropic) value $P_{3c,m}$=0.973 (Fig. 3b corresponding to H_z = 1; the latter being on a slightly larger lattice). Although finite size effects will change these values a little the effect will be small (for monodisperse distributions it was within 0.6% of the infinite system value, see Fig. 3b) and this small shift will be not too different for the different H_z values. We can therefore safely conclude that differential anisotropy can decrease the magma percolation threshold by a significant amount, probably taking it below the 90% level.

7 Conclusions

A few years ago several of us proposed the hypothesis that multibubble coalescence in magmas could be modelled as percolation processes with the basic elements being isotropic bubbles distributed in a power law manner. Near the critical percolation threshold, a small change in vesicularity could lead to a catastrophic decrease in the yield strength, catastrophic breakdown/ fragmentation of the magma such that if the magma is under stress it would explode. We demonstrated the idea with some limited two-dimensional numerical simulations and by comparisons with 2-D data of explosive volcanism including estimates of critical vesicularity values for explosive volcanism ($P_{ex}\approx$0.6–0.7) and also the power law exponent of the distribution of explosive products

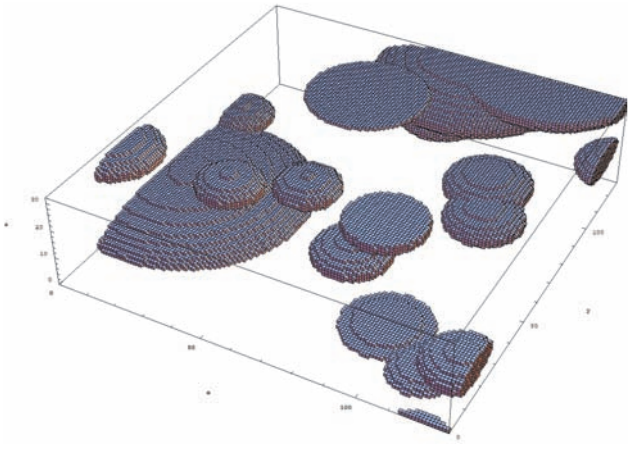

Fig. 8a. The stratified percolation model described in the text is made from disks which are circular with radius L pixels in the horizontal and L^{Hz} in the vertical with power law volume distributions (B_3=0.85). The simulations are on a 128×128×32 grid, with H_z=0.6, (corresponding to an "effective" or "elliptical dimension" of 2+H_z) and the minimum and maximum radius of respectively 10 pixels and 30 pixels (for didactic purposes the smallest bubbles were supressed). Gas bubbles are the opaque shapes.

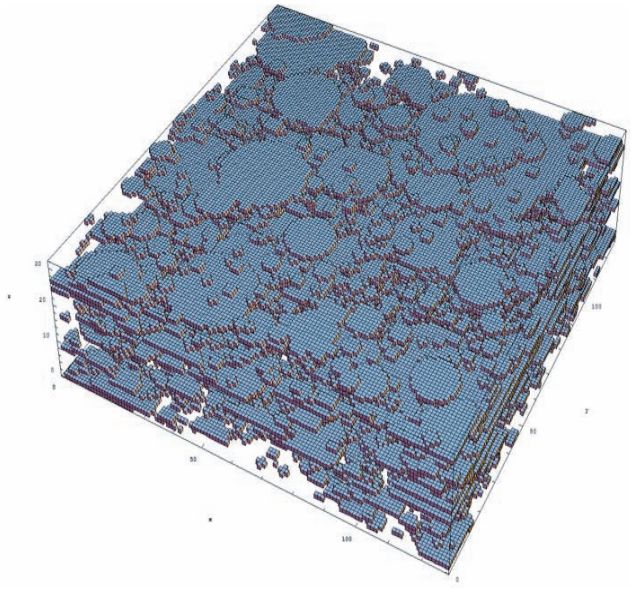

Fig. 8b. The stratified percolation model described in the text made from disks 1 pixel thick in the z (vertical) direction and with power law distributions (B_3=0.85 with an initial bubble distribution with a maximum radius of 10 pixels) in the xy (horizontal plane), corresponding to H_z=0, hence D=2. The simulations are on a 128×128×32 grid, in the figure P=0.152. It is in fact just percolating according to the criterion that percolation occurs in the horizontal plane if and only if a continuous path exists through the bubbles which starts and ends at the same z value (here =10 pixels and not simply on opposite sides as is usually the case, see Fig. 8c).

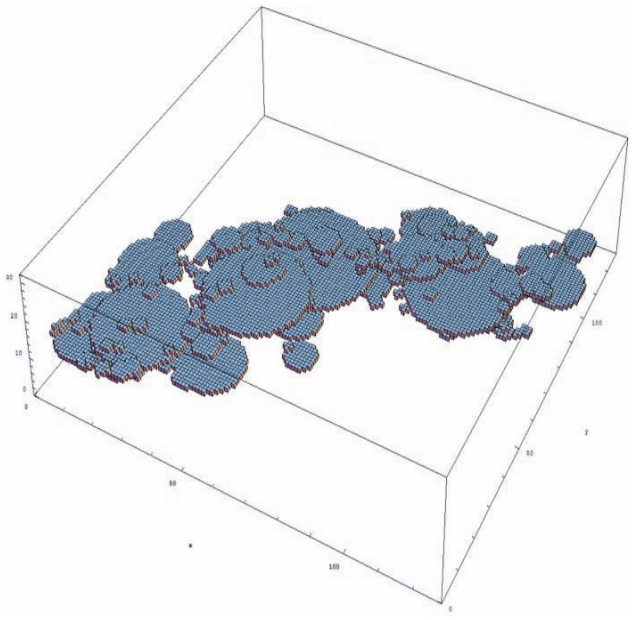

Fig. 8c. The percolating cluster from the realization shown in Fig. 8b. Although only a relatively thin layer of disks participate in the percolating cluster, the possibility of connecting in the vertical direction is enough to reduce the bubble percolation threshold P_c well below the 2-D value ≈0.6 (which we would obtain in the limit of planar disks infinitely thin in the z-direction).

(B_{3f}). This new mechanism could act on its own to trigger an explosion, or – by causing local structural weakening – could act in conjunction with classical pressure surge or strain rate surge mechanisms. Of course, if the magma is not under stress (more likely at low viscosity), then nothing special happens at the percolation point, one has a usual passive degassing, effusive eruption. On the other hand, cases of basaltic Plinian products with very low vesicularities were explained as being the result of a sudden collapse of the bubble network (Gardner et al., 1996).

A serious limitation of the proposed percolation hypothesis was its two-dimensional character: real magmas are three-dimensional, and the change of dimension from two to three leads to several differences, in particular, to the existence of a second "magma" percolation threshold (corresponding to "void" or "Swiss cheese" percolation in the literature). Using the empirical bubble number distribution exponent B_2=0.75 (corresponding to B_3≈0.85), we found that whereas there is a unique 2-D value P_{2c}≈0.7, in 3-D, there are two percolation thresholds: $P_{3c,b}$≈0.25 and $P_{3c,m}$≈0.97. From the simulations, we noted that unlike in 2-D where the fragments have exponent B_{2f}≈0.42, the 3-D value B_{3f}≈1.186 (apparently universal, independent of the bubble B_3) is very close to the observations: B_{3f}≈1.1±0.1 reflecting the dominant effects of multibubble coalescence.

The agreement between the observed and predicted B_{3f} is probably the most convincing direct evidence that

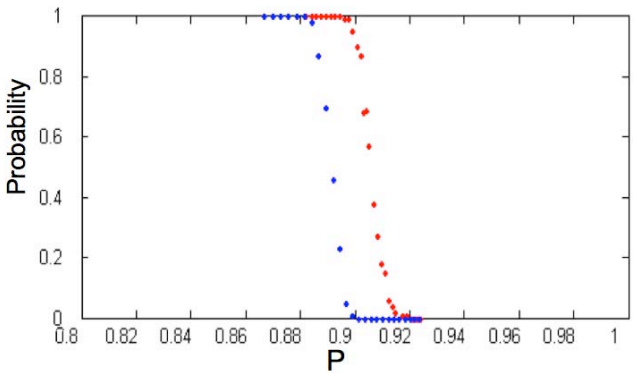

Fig. 9. This shows the effect of varying the vesicularity on the void (magma) percolation probability in the horizontal and vertical directions on a finite 200^3 lattice (100 simulations for each P). With H_z=0.2 blue and red correspond respectively to vertical and horizontal percolation thresholds.

percolation is relevant to explosive volcanism, especially since we numerically showed evidence that the exponent may be observable even at $P\approx0.7$, i.e. somewhat below the critical $P_{3c,m}\approx0.97$ where the magmatic system will automatically disintegrate (theoretically this exponent need only be relevant in the vicinity of $P_{3c,m}$). In contrast, the key weakness of the model in its original form, is that the value $P_{3c,m}\approx0.97$ seems very high for explaining explosive volcanism. However, two caveats should be recognized: a) it may only be necessary for a localized region to reach this high value; if the whole system is under stress then the resulting local breakdown of the magma could trigger a more widespread explosion, b) since remnant fragments of an explosive eruption can be expected to have lower vesicularities than those of the initial exploding system it is not easy to infer vesicularities at the moment of explosion so that we have no good knowledge of the critical P_{ex}.

We therefore explored various ways of achieving lower critical vesicularities including the possible existence of relatively low elastic percolation thresholds and the effects of anisotropy. In the latter case we explicitly considered bubble and magma anisotropy in differentially stratified magmas. We showed that this nonclassical mechanism could reduce $P_{3c,m}$ to around 0.9, with a potential for further reductions. In the case of the elastic properties, we pointed out that critical vesicularities associated with singular rheologies have been studied in the bond and site percolation literature and their (sometimes) lower critical values may be relevant to continuum percolation in visco - elastic magmas.

Clearly, while volcanic eruptions show a wide variety of styles going from pheatomagmatic to Plinian, the role of gas bubbles as a trigger to explosion still remains a challenging question. In any event, given the huge amount of bubble overlap which occurs even at P=0.7, percolation is likely to remain an attractive theoretical framework for understanding highly vesicular magmas involving strong nonlinear bubble-bubble interactions.

It is probable that percolation is only part of the picture; it may be that the magma progressively weakens at higher and higher vesicularity P, but that the trigger for explosion still comes from the classical critical yield strength limit being exceeded by a sudden large overpressure or decompression rate generating large differences between internal and external bubble pressures (typically of 10^6 to 10^9 Pa s) destabilizing the highly viscoelastic surrounding magma which then fragments. Alternatively, the relevant magma percolation threshold is somewhat lower than $P_{3c,m}\approx0.97$ and the mechanism is indeed a rheological singularity at a critical vesicularity P. In any case, the use of a percolation framework at high P surely represents a step towards realism when compared to spherical close-packing and other highly artificial models of high P magmas.

Acknowledgements. This research has been supported by the National Sciences and Engineering Research Council of Canada. M. Carrier-Nunes is grateful for a GEOTOP fellowship for this project. GEOTOP Publication no. 2007-0056.

Edited by: A. Tarquis
Reviewed by: two anonymous referees

References

Aldibirov, M.: A model for viscous magma fragmentation during volcanic blasts, Bull. Volcanol., 56, 459–465, 1994.

Aldibirov, M. and Dingwell, D. B.: Magma fragmentation by rapid decompression, Nature, 380, 146–148, 1996.

Arbabi, S. and Sahimi, M.: Elastic properties of three-dimensional percolation networks with stretching and bond-bending forces, Phys. Rev. B, 38, 7173–7176, 1988.

Arbabi, S. and Sahimi, M.: Mechanics of disordered solids. I. Percolation on elastic networks with central forces., Phys. Rev. B, 47, 695–702, 1993.

Balberg, I.: "Universal" percolation-threshold limits in the continuum, Phys. Rev. B, 31, 4053–4055, 1985.

ben-Avraham, D. and Havlin, S.: Diffusion and reactions in fractals and disordered systems, 316 pp., Cambridge University Press, Cambridge, 2000.

Craciun, F., Galassi, C., and Roncari, E.: Experimental evidence for similar critical behaviour of elastic modulus and electric conductivity in porous ceramic materials, Europhys. Lett., 41, 55–60, 1998.

de Dreuzy, J.-R., Davy, P., and Bour, O.: Percolation parameter and percolation-threshold estimates for three-dimensional random ellipses with widely scattered distributions of eccentricity and size, Phys. Rev. E, 62, 5948–5952, 2000.

Den Nijs, M. P. M.: A relation between the temperature exponents of the eight vertex and q-state Potts models, J. Phys., 12, 1857–1871, 1979.

Dingwell, D. B. and Webb, S. L.: Structural relaxation in siloicate melts and non-Newtonian melt rheology in igneous processes, Phys. Chem. Miner., 16, 508–516, 1989.

Essam, J. W., Gaunt, D. S., and Guttmann, A. J.: Percolation theory at the critical dimension, J. Phys. A, Math. Gen., 11, 1983–1990, 1978.

Gaonac'h, H., Stix, J., and Lovejoy, S.: Scaling effects on vesicle shape, size and heterogeneity of lavas from Mount Etna, J. Volcanology Geothermal Res., 74, 131–153, 1996a.

Gaonac'h, H., Lovejoy, S., Stix, J., and Schertzer, D.: A scaling growth model for bubbles in basaltic lava flows, Earth Planet. Sci. Lett., 139, 395–409, 1996b.

Gaonac'h, H., Lovejoy, S., and Schertzer, D.: Percolating Magmas and explosive volcanism, Geophys. Res. Lett., 30, 1559–1563, 2003.

Gardner, J. E., Thomas, R. M. E., Jaupart, C., and Tait, S.: Fragmentation of magma during Plinian volcanic eruptions, Bull. Volcanology, 58, 144–162, 1996.

Gonnermann, H. M. and Manga, M.: Explosive volcanism may not be an inevitable consequence of magma fragmentation, Nature, 426, 432–435, 2003.

Grassberger, P.: On the behaviour of the general epidemic process and dynamical percolation, Math. Biosci., 63, 157–161, 1983.

Ichihara, M., Rittel, D., and Sturtevant, B.: Fragmentation of a porous viscoelastic material: Implications to magma fragmentation, J. Geophys. Res., 107(B10), 2229, doi:10.1029/2001JB000591, 2002.

Jan, N. and Stauffer, D.: Random site percolation in three dimensions, Int. J. Mod. Phys., C9, 341–347, 1998.

Kaminski, E. and Jaupart, C.: The size distribution of pyroclasts and the fragmentation sequence in explosive volcanic eruptions, J Geophys Res., 103, 29 759–29 779, 1998.

Klug, C. and Cashman, K. V.: Vesiculation of May 18, 1980, Mount St. Helens magma, Geology, 22, 468–472, 1994.

Klug, C., Cashman, K. V., and Bacon, C. R.: Structure and physical characteristics of pumice from the climatic eruption of Mount Mazama (Crater Lake) Oregon, Bull. Volcanology, 64, 486–501, 2002.

Kueppers, U., Perugini, D., and Dingwell, D. B.: "Explosive energy" during volcanic eruptions from fractal analysis of pyroclasts, Earth Planet. Sci. Lett., 248, 800–807, 2006.

Lorenz, C. M. and Ziff, R. M.: Precise determination of the bond percolation thresholds and finite-size scaling corrections for the sc, fcc and bcc lattices, Phys. Rev. E, 57, 230–236, 1998.

Lovejoy, S., Gaonac'h, H., and Schertzer, D.: Bubble distributions and dynamics: the expansion-coalescence equation, J. Geophys. Res. (Solid Earth), 109, B, 11203, doi:10.1029/2003JB002823, 2004.

Meille, S. and Garboczi, E. J.: Llinear elastic properties of 2D and 3D models of porous materials made froom elgongated objects, Modelling Simul. Mater. Sci. Eng., 9, 371–390, 2001.

Namiki, M. and Manga, M.: Response of a bubble bearing viscoelastic fluid to rapid decompression: implications for explosive volcanic eruptions, Earth Planet. Sci. Lett., 236, 269–284, 2005.

Namiki, M. and Manga, M.: Influence of decompression rate on the expansion velocity and expansion style of bubbly fluids, J. Geophys. Res., 111, B11 208–B11 225, 2006.

Papale, P.: Strain-induced magma fragmentation in explosive eruptions, Nature, 397, 425–428, 1999.

Polacci, M., Papale, P., and Rosi, M.: Textural heterogeneities in pumices from the climactic eruption of Mount Pinatubo,15 June 1991,and implications for magma ascent dynamics, Bull. Volcanology, 63, 83–97, 2001.

Quintanilla, J.: Measurement of the percolation threshold for fully penetrable disks of different radii, Phys. Rev. E, 63, 061108, 2001.

Rintoul, M. D.: Precise determination of the void percolation threshold for two distributions of of overlapping sphere, Phys. Rev. E, 62, 68–72, 2000.

Rintoul, M. D. and Torquato, S.: Precise determination of the critical threshold and exponents in a three-dimensional continuum percolation model, J. Phys. A, Math. Gen., 30, L585–L592, 1997.

Sahimi, M. and Arbabi, S.: Mechanics of disordered solids. II. Percolation on elastic networks with bond-bending forces, Phys. Rev. B, 47, 703–712, 1993.

Scher, H. and Zallen, R.: Critical density in percolation processes, J. Chem. Phys., 53, 3759–3761, 1970.

Schertzer, D. and Lovejoy, S.: Generalised scale invariance in turbulent phenomena, Physico-Chemical Hydrodynamics Journal, 6, 623–635, 1985.

Sparks, R. S. J.: The dynamics of bubble formation and growth in magmas, J. Volcanology Geothermal Res., 3, 1–37, 1978.

Spieler, O., Kennedy, B., Kueppers, U., Dingwell, D. B., Scheu, B., and Taddeuccfi, J.: The fragmentation threshold of pyroclastic rocks, Earth Planet. Sci. Lett., 226, 139–148, 2004.

Stauffer, D.: Introduction to percolation Theory, Taylor & Francis, London, Philadelphia, 1985.

Thomas, N., Jaupart, C., and Vergniolle, S.: On the vesicularity of pumice, J. Geophys. Res., 99, 15 633–615 644, 1994.

Yi, Y. B.: Void percolation and conduction of overlapping ellipsoids, Phys. Rev. E, 74, 031112-031111-031112-031116, 2006.

Zhang, Y.: A criterion for the fragmentation of bubbly magma based on brittle failure theory, Nature, 402, 648–650, 1999.